The Plant Cell, Vol. 21: 2750–2761, September 2009, www.plantcell.org © 2009 American Society of Plant Biologists

The *Arabidopsis* Nitrate Transporter NRT1.7, Expressed in Phloem, Is Responsible for Source-to-Sink Remobilization of Nitrate [W][OA]

Shu-Chun Fan,[a,b] Choun-Sea Lin,[b,1] Po-Kai Hsu,[a,b] Shan-Hua Lin,[b] and Yi-Fang Tsay[b,2]

[a] Graduate Institute of Life Sciences, National Defense Medical Center, Taipei 112, Taiwan
[b] Institute of Molecular Biology, Academia Sinica, Taipei 115, Taiwan

Several quantitative trait locus analyses have suggested that grain yield and nitrogen use efficiency are well correlated with nitrate storage capacity and efficient remobilization. This study of the *Arabidopsis thaliana* nitrate transporter NRT1.7 provides new insights into nitrate remobilization. Immunoblots, quantitative RT-PCR, β-glucuronidase reporter analysis, and immunolocalization indicated that *NRT1.7* is expressed in the phloem of the leaf minor vein and that its expression levels increase coincidentally with the source strength of the leaf. In *nrt1.7* mutants, more nitrate was present in the older leaves, less $^{15}NO_3^-$ spotted on old leaves was remobilized into N-demanding tissues, and less nitrate was detected in the phloem exudates of old leaves. These data indicate that NRT1.7 is responsible for phloem loading of nitrate in the source leaf to allow nitrate transport out of older leaves and into younger leaves. Interestingly, *nrt1.7* mutants showed growth retardation when external nitrogen was depleted. We conclude that (1) nitrate itself, in addition to organic forms of nitrogen, is remobilized, (2) nitrate remobilization is important to sustain vigorous growth during nitrogen deficiency, and (3) source-to-sink remobilization of nitrate is mediated by phloem.

INTRODUCTION

Nitrogen fertilizer is one of the most expensive nutrients to supply. Approximately 85 to 90 million metric tons of nitrogenous fertilizers are applied worldwide annually (Good et al., 2004). However, 50 to 70% of the applied nitrogen is lost from the plant soil system and causes water pollution (Peoples et al., 1995). Therefore, improving nitrogen use efficiency (NUE) is important to reduce the cost of crop production as well as environmental damage. Nitrogen remobilization is one of the key steps to improve NUE (Mickelson et al., 2003; Masclaux-Daubresse et al., 2008).

When plants encounter nutrient deficiency, nitrogen, a mobile element, can be recycled from older to younger leaves to sustain the growth of developing tissues, similar to remobilization of potassium and phosphorus. N remobilization occurs not only from leaf to leaf during the vegetative stage but also from leaf to seeds during the reproductive stage (Simpson et al., 1983; Wendler et al., 1995; Rossato et al., 2001; Schiltz et al., 2005). High nutrient demand during the reproductive stage cannot be satisfied by N uptake, and nitrogen recycled from senescent tissue plays an important role in sustaining grain production. For example, in wheat (*Triticum aestivum*) and maize (*Zea mays*), the contribution of leaf N remobilization to grain production is cultivar dependent, varying from 50 to 90% (Kichey et al., 2007).

Several studies have showed that N remobilization is associated with increased proteolysis activity and senescence in the source organ, and N import into developing tissues such as seeds is derived from the remobilization of amino acids liberated by proteolysis of proteins synthesized during the vegetative phase (Hortensteiner and Feller, 2002; Good et al., 2004; Jukanti and Fischer, 2008; Masclaux-Daubresse et al., 2008). Ribulose-1,5-bisphosphate carboxylase/oxygenase (Rubisco; accounting for ~50% of the total soluble protein in a leaf), light-harvesting complex II, and vegetative storage proteins are major sources of organic N for remobilization (Matile et al., 1992; Mitsuhashi et al., 1992; Lansing and Franceschi, 2000). Rubisco proteolysis is proposed to be initiated by a cleavage via the action of reactive oxygen species to generate a 37- and 16-kD fragment (Ishida et al., 1997). Subsequently, endopeptidases and exopeptidases are required for the complete hydrolysis of Rubisco (Roulin and Feller, 1998; Kato et al., 2004). Depending on the plant species, Asn or Gln is the preferred N compound exported from the senescing leaf (Rochat and Boutin, 1991; Caputo and Barneix, 1997).

In addition to amino acids, inorganic nitrogen in the form of nitrate might also be remobilized among different organs. Nitrate and ammonium are two major nitrogen sources that plants acquire from soil. Due to its toxic effect, ammonium taken into plants has to be assimilated immediately and converted into organic nitrogen. However, significant amounts of the nitrate taken into plants can be stored in vacuoles and recirculated after storage (Rossato et al., 2001). A study by Richard-Molard et al.

[1] Current address: Agricultural Biotechnology Research Center, Academia Sinica, Taipei 115, Taiwan.
[2] Address correspondence to yftsay@gate.sinica.edu.tw.
The author responsible for distribution of materials integral to the findings presented in this article in accordance with the policy described in the Instructions for Authors (www.plantcell.org) is: Yi-Fang Tsay (yftsay@gate.sinica.edu.tw).
[W]Online version contains Web-only data.
[OA]Open access articles can be viewed online without a subscription.
www.plantcell.org/cgi/doi/10.1105/tpc.109.067603

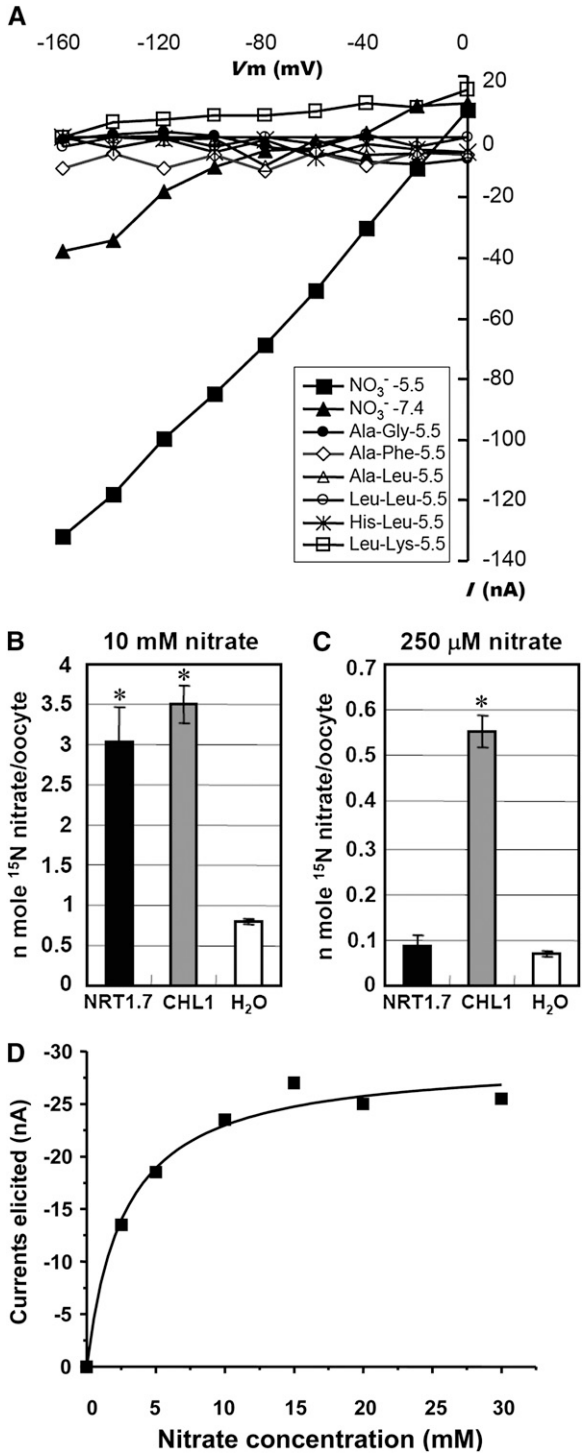

Figure 1. NRT1.7 Is a Low-Affinity Nitrate Transporter.

(A) Substrate specificity of NRT1.7. *NRT1.7* cRNA-injected oocytes were voltage clamped at −60 mV and stepped to a test voltage between 0 and −160 mV for 300 ms, in increments of −20 mV. The currents (*I*) shown here are the differences between the currents flowing at +300 ms in the presence and in the absence of 10 mM nitrate or 10 mM dipeptides at the pH indicated. Similar results were obtained from two other oocytes from different frogs.

(2008) showed that an *Arabidopsis thaliana* line that exhibited higher nitrate storage capacities coped better with nitrate starvation. In addition, quantitative trait locus (QTL) analysis of maize and barley (*Hordeum vulgare*) also showed that increased productivity or grain protein content is probably associated with their ability to accumulate higher amounts of nitrate in their leaves during vegetative growth and then to efficiently remobilize the stored nitrate during grain filling (Hirel et al., 2001; Mickelson et al., 2003). Although several studies have shown that nitrate remobilization is important to increase grain yield and withstand nitrogen deprivation, little is known about how nitrate is remobilized.

Three types of nitrate transporters, NRT1, NRT2, and CLC (chloride channel family), have been identified in higher plants and play diverse roles in nitrate balance in the plant (Hechenberger et al., 1996; Forde, 2000; Orsel et al., 2002; Tsay et al., 2007). *Arabidopsis* CLCa, a proton-nitrate exchanger located in tonoplasts, mediates nitrate accumulation in vacuoles (De Angeli et al., 2006). NRT1 and NRT2 comprise families of proton-coupled transporters with 53 and 7 members, respectively, in *Arabidopsis*. Four of them, *Arabidopsis* NRT1.1, NRT1.2, NRT2.1, and NRT2.2, participate in nitrate uptake (Tsay et al., 1993; Wang et al., 1998; Huang et al., 1999; Liu et al., 1999; Filleur et al., 2001; Little et al., 2005; Li et al., 2007) using a proton gradient as a driving force to transport nitrate from the soil into plant cells. On the other hand, both NAXT1 (a NRT1 transporter; Segonzac et al., 2007) and NRT1.5 mediate nitrate efflux, and NRT1.5 is involved in xylem loading for root-to-shoot transport of nitrate (Lin et al., 2008). NRT1.4 regulates leaf nitrate homeostasis (Chiu et al., 2004). NRT2.7 is involved in seed nitrate storage (Chopin et al., 2007), and NRT1.6 is involved in delivering nitrate from maternal tissue to developing embryos (Almagro et al., 2008). Nitrate can be stored, and it is important to find out how the stored nitrate is retrieved to withstand nitrogen deficiency and to sustain high nitrogen demand in the reproductive stage. In this study, we found that the *Arabidopsis* NRT1 transporter NRT1.7 is involved in nitrate remobilization. The

(B) Low-affinity nitrate uptake activity of *NRT1.7*-, *CHL1*-, or water-injected oocytes. Oocytes were incubated with 10 mM ^{15}N-nitrate at pH 5.5 for 2 h. ^{15}N retained in the oocytes was measured as described in Methods. Values are means ± SD (n = 5)

(C) High-affinity nitrate uptake activity of *NRT1.7*-, *CHL1*-, or water-injected oocytes. Oocytes were incubated with 250 μM ^{15}N-nitrate at pH 5.5 for 1 h. Values are means ± SD (n = 10, 9, and 6 for *NRT1.7*-, *CHL1*-, and water-injected oocytes, respectively). For **(B)** and **(C)**, similar results were obtained using three other frogs. *, Significant difference at $P < 0.001$ compared with the water-injected control.

(D) Kinetics of nitrate-elicited currents in a single *NRT1.7* cRNA-injected oocyte. The oocyte was voltage clamped at −60 mV. The inward current elicited by different concentrations of nitrate at pH 5.5 was plotted as a function of the external nitrate concentration. In this particular experiment, the K_m, calculated by fitting to the Michaelis-Menton equation using a nonlinear least squares methods in the ORIGIN 5.0 program (Microcal Software; GE Healthcare), was 2.7 ± 0.6 mM. The example shown is representative of the results from six oocytes from four different frogs.

properties of NRT1.7 indicate that nitrate remobilization from source to sink tissues is mediated by phloem transport.

RESULTS

NRT1.7 Encodes a Low-Affinity Nitrate Transporter

In *Arabidopsis*, there are 53 NRT1 (PTR) genes, some of which are known to transport nitrate, while others transport dipeptides. The protein sequence of NRT1.7 shows 33, 30, 34, 36, 33, 69, and 35% identity with that of NRT1.1, NRT1.2, NRT1.3, NRT1.4, NRT1.5 NRT1.6, and NAXT1, respectively, and 40, 37, and 35% identity with PTR1, PTR2, and PTR3, respectively (see Supplemental Figure 1 online). To determine the substrate specificity of NRT1.7, in vitro–synthesized cRNA was injected into *Xenopus laevis* oocytes for electrophysiological analysis. After 2 d of incubation in ND96, oocytes were voltage clamped at −60 mV and then subjected to 300-ms voltage pulses from 0 to ~160 mV in −20-mV increments. *NRT1.7*-injected oocytes responded to 10 mM nitrate at pH 5.5 with inward currents. The inward currents were elicited by nitrate but not by the dipeptides tested (Figure 1A). The current-voltage kinetics of NRT1.7 are similar to those of other nitrate transporters in the NRT1/PTR family (Huang et al., 1999; Chiu et al., 2004, Almagro et al., 2008; Lin et al., 2008). The current elicited by nitrate was pH dependent, with little or no current detected when exposed to nitrate at pH 7.4, suggesting that a proton gradient is important for nitrate transport. The pH dependence of nitrate elicited currents suggested that NRT1.7 might be a proton-coupled nitrate transporter.

Most of the nitrate transporters in the NRT1 (PTR1) family function as low-affinity transporters with exception of NRT1.1 (CHL1), which is a dual-affinity nitrate transporter (Wang et al., 1998; Liu et al., 1999; Liu and Tsay, 2003). To determine the affinity of NRT1.7, the high- and low-affinity nitrate transport activities of cRNA-injected oocytes were assessed by incubating the oocytes with 10 mM ^{15}N-nitrate for 2 h or 250 μM ^{15}N-nitrate for 1 h, respectively. Consistent with the previous data, *CHL1* cRNA-injected oocytes showed both high- and low-affinity nitrate transport, while *NRT1.7* cRNA-injected oocytes were found to take up nitrate only with low affinity (Figures 1B and 1C). The K_m of NRT1.7 for nitrate was calculated from currents elicited at −60 mV by different concentrations of nitrate. The average K_m calculated from six independent oocytes was 2.8 ± 0.9 mM.

NRT1.7 Is Expressed in Phloem Tissue of Older Leaves

Microarray data from the public resource *Arabidopsis thaliana* Expression Database CSB.DB shows that little or no expression of *NRT1.7* can be detected in root and that transcription levels in leaves increase as leaves age (see Supplemental Figure 2A online). The differential expression of NRT1.7 in old and young leaves was further confirmed here by immunoblot analysis (Figure 2A). Using BiP (Luminal Binding Protein) as loading control, the NRT1.7 protein level in the oldest leaves was ~25 times higher than that in the youngest leaves. In addition, the leaves were separated into distal lamina, proximal lamina, and central part including midrib and petiole for quantitative RT-PCR

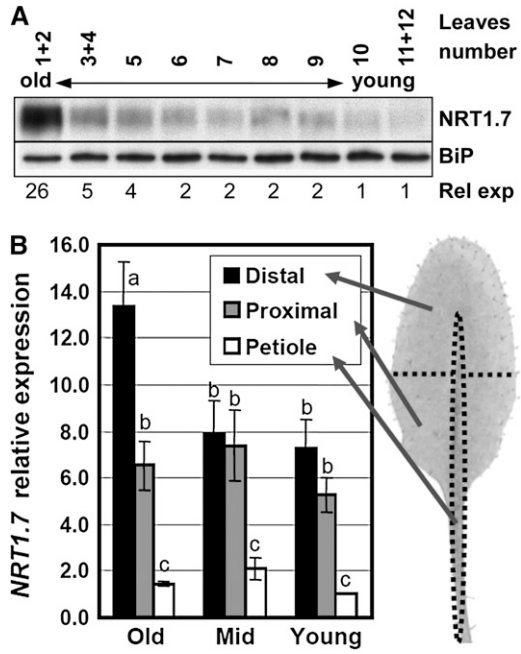

Figure 2. NRT1.7 Is Predominantly Expressed in Old Leaves.

(A) High levels of NRT1.7 protein in older leaves. Protein from individual leaves of 23-d-old plants were separated by SDS-PAGE, transferred to a polyvinylidene fluoride membrane (Bio-Rad), and hybridized with NRT1.7-specific antibody. The top part of the same membrane was hybridized with BiP antibodies as loading control. The values of NRT1.7 protein levels normalized to BiP level, with the young leaf levels set at 1, are indicated below the blot. Similar results were found in three biological repeats.

(B) Quantitative RT-PCR analysis of *NRT1.7* expression. The leaves were separated into distal lamina, proximal lamina, and central part, including midrib and petiole, for RNA isolation. *NRT1.7* was preferentially expressed in the distal part of older leaves. The relative expression level shown here is the expression of *NRT1.7* normalized to that of *UBQ10*. Values are means ± SE of four biological repeats. The statistically significant differences are indicated by different letters ($P < 0.01$).

analysis. The *NRT1.7* mRNA level was higher in the distal lamina of older leaves (Figure 2B).

To confirm the *NRT1.7* expression pattern, 13 independent transgenic lines expressing β-glucuronidase (GUS) driven by *NRT1.7* promoter were analyzed. Consistent with immunoblot and RT-PCR results, GUS staining was stronger in the older leaves, while little or no staining was detected in the younger leaves. In between, there were a few transition leaves with GUS staining extending from the tip to the base of the leaves (indicated by arrows in Figure 3A). A similar pattern was found in all of the 13 independent lines. Source strength is known to develop in the tip to base direction (Turgeon and Webb, 1973). Preferential expression of NRT1.7 in the distal part of transition leaves suggests that NRT1.7 could be involved in exporting nutrient out of the matured and aged leaves.

Closer examination of the GUS staining indicated that NRT1.7 was mainly expressed in minor veins (Figure 3B). In addition, microscopy analysis of the leaf sections indicated that the expression was restricted to the sieve element and companion

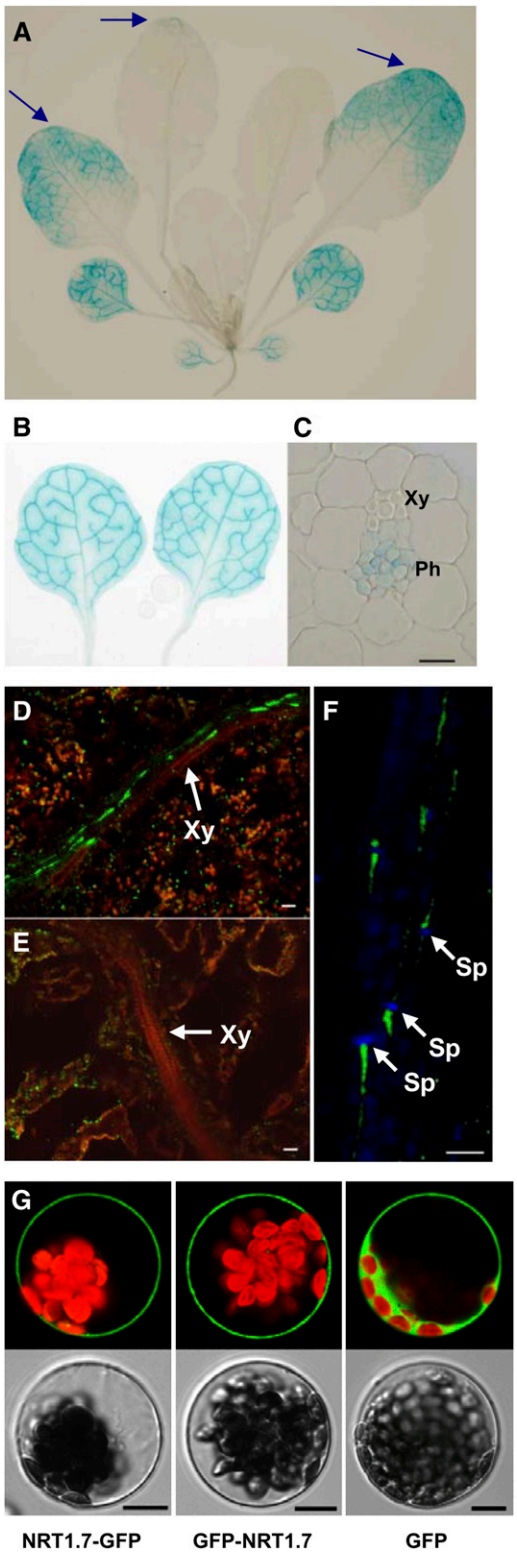

Figure 3. High Level of NRT1.7 Expression Is Detected in Phloem.

(A) Histochemical localization of GUS activity in 28-d-old p*NRT1.7*-GUS plants. In the sink-to-source transition leaves indicated by arrows, *NRT1.7* expression gradually increased from distal to basal parts of the lamina. GUS staining patterns were consistent in 13 independent transgenic lines.

(B) GUS activity in minor vein of a 32-d-old p*NRT1.7*-GUS plant.

(C) Cross section of minor veins of a p*NRT1.7*-GUS plant. GUS activity was located at the sieve element and companion cell complex. Xy, xylem, Ph, phloem.

(D) to **(F)** Immunodetection of NRT1.7 protein in whole-mount hybridization. Older leaves of Col wild type (**[D]** and **[F]**) or *nrt1.7-2* mutant **(E)** were labeled with anti-NRT1.7 antiserum and with fluorescence-conjugated goat anti-rabbit antiserum. Images were taken by confocal laser scanning microscopy. Green fluorescence, NRT1.7; red color, autofluorescence; blue color, sieve plates stained with aniline blue. Green immunosignal was detected in the wild type **(D)** but not in *nrt1.7* mutant **(E)**. Xy, xylem, Sp, sieve plate.

(G) Subcellular localization of NRT1.7 and GFP fusion protein in *Arabidopsis* protoplasts. Confocal laser scanning microscopy pictures (top panels) and corresponding bright-field images (bottom panels) of *Arabidopsis* protoplasts transiently expressing NRT1.7-GFP, GFP-NRT1.7, or GFP alone.

Bars = 10 μm.

cell complex (Figure 3C). Whole-mount immunostaining was used to confirm the NRT1.7 protein location. Green fluorescence of anti-NRT1.7 antiserum labeling was detected in vascular tissues of the wild type (Figure 3D) but not *nrt1.7-2* mutant (Figure 3E), and green fluorescence was found to be parallel to the xylem. In addition, as shown in Figure 3F and Supplemental Figure 3 online, when sieve plates were stained with aniline blue, green fluorescence was found to be next to the sieve plates. Independent evidence of GUS reporter assay and immunolocalization showed that NRT1.7 is present in the companion cell and sieve element complex. This expression pattern of NRT1.7 suggests that it might be involved in phloem loading, particularly in mature leaves.

NRT1.7 Is Localized to the Plasma Membrane

To investigate the subcellular localization of NRT1.7, green fluorescent protein (GFP) fused either N-terminally or C-terminally to NRT1.7 was transiently expressed in *Arabidopsis* protoplasts under the control of the cauliflower mosaic virus 35S promoter. Green fluorescence was seen in cytoplasm in the GFP control, while the green fluorescence of NRT1.7-GFP and GFP-NRT1.7 (Figure 3G) was detected as a fine ring at the cell periphery, external to the chloroplasts, indicating that NRT1.7 is localized in the plasma membrane.

Expression of *NRT1.7* Is Diurnally Regulated and Temporally Opposite to That of *NIA2*

Shoots of plants grown for 20 d under a 12-h photoperiod were collected to determine the diurnal changes in the expression of *NRT1.7* and nitrate reductase gene *NIA2*. Quantitative PCR analysis indicated that the *NRT1.7* transcript level increased gradually during the light period, reached a maximum in the early part of the dark period, and declined thereafter (Figure 4). By contrast, *NIA2* transcripts decreased during the light period, were minimal at the late stage of the light period, and then

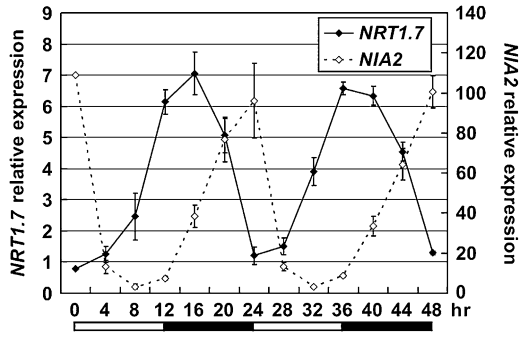

Figure 4. *NRT1.7* Expression Is Diurnally Regulated.

RNA from shoots of 20-d-old wild-type (Col) plants grown under 12-h photoperiod were used for quantitative RT-PCR. The relative expression levels are the expression of *NRT1.7* and *NIA2* normalized to the expression of *UBQ10*. Values are means ± SE of five biological repeats at each time point except time 0 with only two biological repeats.

increased gradually during the dark period. This opposite temporal pattern of *NRT1.7* and *NIA2* mRNA levels suggests that *NRT1.7* is needed when nitrate reductase activity is low.

nrt1.7 Null Mutants Accumulate a Higher Amount of Nitrate in Older Leaves

To determine the in vivo function of *NRT1.7*, two T-DNA insertion mutants were isolated. Mutant *nrt1.7-1* in the Wassilewskija (Ws) ecotype was isolated by PCR-based screening (Krysan et al., 1999), and a second mutant, *nrt1.7-2*, SALK_053264, in the Columbia (Col) ecotype was obtained from the ABRC (Alonso et al., 2003). In *nrt1.7-1* and *nrt1.7-2* mutants, one copy and three contiguous copies of T-DNA, respectively, were inserted in the second intron of *NRT1.7* gene (Figure 5A). No expression of *NRT1.7* mRNA and protein could be detected by RT-PCR (data not shown) and immunoblot analysis (Figure 5B) showing that both are null mutants.

The nitrate content in each leaf was analyzed in the wild type and mutants. Compared with the wild type, higher amounts of nitrate accumulated in older leaves of the mutants (Figures 5C and 5D; see Supplemental Figure 4 online). Preferential expression of *NRT1.7* in older leaves and accumulation of nitrate in the older leaves of the mutants suggest that NRT1.7 is responsible for remobilizing nitrate from the older leaves to other tissues.

nrt1.7 Mutants Are Defective in Remobilizing ^{15}N-Nitrate from Older Leaves to Younger Leaves

That NRT1.7 functions in nitrate remobilization was further confirmed by a ^{15}N-nitrate spotting experiment. ^{15}N-nitrate was spotted on distal parts of the oldest nonsenescent leaf, and 20 h after spotting, ^{15}N content of different leaves and organs was analyzed. In the wild type, ^{15}N-nitrate spotted on the old leaf moved to younger leaves; in the mutants, little or no ^{15}N could be found in the young leaves (Figures 6A and 6B). In contrast with sucrose export studies (Kiefer and Slusarenko, 2003), ^{15}N remobilization does not show a vertical transport pattern (orthostichy). The amount of ^{15}N exported out of the spotted leaf in the mutants was 20 to 40% of the wild-type levels. These data indicate that the nitrate transporter NRT1.7 is responsible for remobilizing nitrate from older leaves to N-demanding tissues, such as young leaves.

Since NRT1.7 is expressed in the phloem of older leaves, the amount of nitrate in the phloem sap was compared between the wild type and mutants. In a slight modification of an older protocol (Deeken et al., 2008), the third and fourth leaves were cut, recut in EDTA buffer, washed, and then placed into tubes with 200 μL of EDTA buffer. After phloem bleeding for 1 h, the buffer solution, which contained diluted phloem sap, was used for composition analyses. The glucose content in the phloem exudates was lower than the detection limit (50 n mole/g fresh weight [FW]), suggesting that the contamination of damaged cell extract in the exudates was low. Nitrate content in the exudates was 159.9 ± 9.7 n mole/g FW in Ws, 96.8 ± 7.4 in *nrt1.7-1*, 193.2 ± 11.5 in Col, and 123.9 ± 5.0 in *nrt1.7-2* (Figure 6C), indicating that compared with the wild type, the nitrate content of phloem exudate in *nrt1.7* mutants decreased 35 to 40%. Other types of transporters or loading mechanisms could be responsible for the remaining nitrate detected in the phloem sap of the *nrt1.7* mutants. The sucrose content in the mutants is comparable to the values of their corresponding wild types (Figure 6D), suggesting that reduced nitrate content in the mutants is not due to reduced exudation rate of phloem sap in the mutants. Probably due to the differences in plant species and leaf ages, the sucrose-to-nitrate ratio of phloem exudates in this study is ~10, which is lower than the ratio of 30 observed in wheat (Hayashi and Chino, 1986).

Growth Retardation in *nrt1.7* Mutants during Nitrogen Starvation

Under nutrient-sufficient conditions, no growth difference was seen between mutants and the wild type. However, when plants were starved of nitrogen at an early stage (10 d after germination), both *nrt1.7* mutants showed growth retardation compared with the wild type (Figure 7A). When compared with the wild type grown in the same pots, the rosettes in the mutants were ~30% smaller in diameter (Figures 7B and 7C). Quantitative RT-PCR analysis revealed that *NRT1.7* expression in shoot was induced by nitrogen starvation (Figure 7D; see Supplemental Figure 6 online). The growth retardation found in mutants and the enhanced expression of *NRT1.7* during nitrate starvation suggest that nitrate remobilization is important to sustain vigorous growth under nitrogen starvation conditions.

DISCUSSION

Arabidopsis NRT1.7 Mediates Phloem Loading of Nitrate in Source Leaves to Remobilize Nitrate from Older Leaves to Nitrogen-Demanding Tissues

Functional analysis in *Xenopus* oocytes showed that NRT1.7 is a pure low-affinity nitrate transporter, with a K_m of ~2.8 mM in oocytes. A GFP fusion study showed that NRT1.7 is located in the plasma membrane. Immunoblot analysis showed that

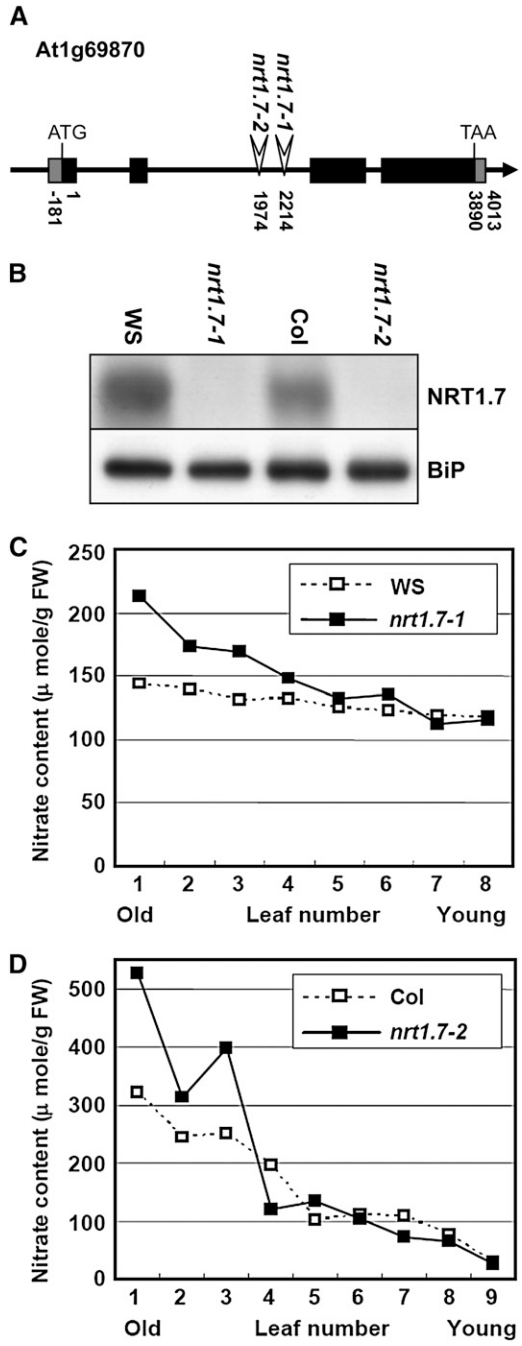

Figure 5. Nitrate Accumulated in Older Leaves of *nrt1.7* Mutants.

(A) Schematic map of the *nrt1.7-1* and *nrt1.7-2* mutants. Both mutants carry the T-DNA insertion in the second intron of the *NRT1.7* gene. The black and white boxes represent the coding and untranslated regions, respectively. The number indicated the insertion site of two mutants with start codon as 1 and stop codon as 3890.

(B) Immunoblot analysis of NRT1.7 protein levels in the wild-type and in homozygous *nrt1.7* mutants. Total membrane proteins (10 μg) from two wild types and two mutants were separated by SDS-PAGE and analyzed as described in the legend of Figure 2A. Both *nrt1.7* lines are null mutants.

NRT1.7 is mainly expressed in older leaves. GUS staining analysis and immunolocalization further indicated that NRT1.7 is expressed in the companion cell and sieve element complex of the minor vein. Compared with the wild type, more nitrate accumulated in older leaves of *nrt1.7* mutants, a defect in nitrate remobilization that was further confirmed by ^{15}N-nitrate tracing assay, which showed that ^{15}N-nitrate spotted on the oldest leaf could be remobilized to younger leaves in the wild type but not in *nrt1.7* mutants. In addition, the nitrate content of phloem exudates from older leaves of *nrt1.7* mutants fell. Taken together, these data suggest that NRT1.7 in source leaves is involved in loading nitrate into the phloem for remobilization.

NRT1.7, a plasma membrane transporter of the sieve element/companion cell complex, was involved in moving excess nitrate from older leaves into developing tissues, indicating that apoplastic phloem loading is responsible for nitrate remobilization. Some studies have suggested that nitrate cannot be detected in phloem sap (Pate et al., 1975; Hocking, 1980); however, using a different detection method (e.g., liquid chromatography), some studies found 1.9 to 8.1 mM nitrate in phloem sap of plants grown with sufficient nitrate (Smith and Milburn, 1980; Hayashi and Chino, 1985, 1986; Allen and Smith, 1986).

Nitrate is known to be stored in vacuoles. Therefore, excess nitrate stored in mesophyll cells needs to be transported across the tonoplast and then the plasma membrane to be loaded apoplastically into the phloem. These three steps of transport (across tonoplast of mesophyll cell, plasma membrane of mesophyll cell, and plasma membrane of companion cell and sieve element) need to be coordinated to remobilize nitrate efficiently. Genes involved in the first two steps have not been identified. The reduced nitrate content in phloem sap and reduced $^{15}NO_3^-$ remobilization in *nrt1.7* mutants suggest that transport across the plasma membrane of companion cell and sieve element is a rate-limiting step for nitrate remobilization.

Nitrate Remobilization Is Important for Sustained Growth under Nitrogen Starvation

NRT1.7 is involved in nitrate remobilization from the old leaf. Mutants of *nrt1.7* defective in this process had retarded growth when the plants encountered long-term severe nitrogen deficiency during vegetative growth, indicating that internal nitrate remobilization between leaves was important for plants to cope with nitrogen deficiency and the importance of enhanced NUE for maximum growth. Consistent with this, by comparing nitrogen contents and growth of two *Arabidopsis* lines in response to nitrogen starvation, Richard-Molard et al. (2008) found that the line with higher nitrate storage capacity prior to nitrate starvation coped better with nitrate starvation. Our study of NRT1.7

(C) and **(D)** More nitrate accumulated in older leaves of mutants. Individual leaves were collected and nitrate content measured from 28- to 32-d-old plants grown in soil with full nutrient under 16-h photoperiods. The wild type and mutant were grown in the same pot for comparison. Similar results were observed in three different pairs of Ws and *nrt1.7-1* comparisons and three of Col and *nrt1.7-2*.

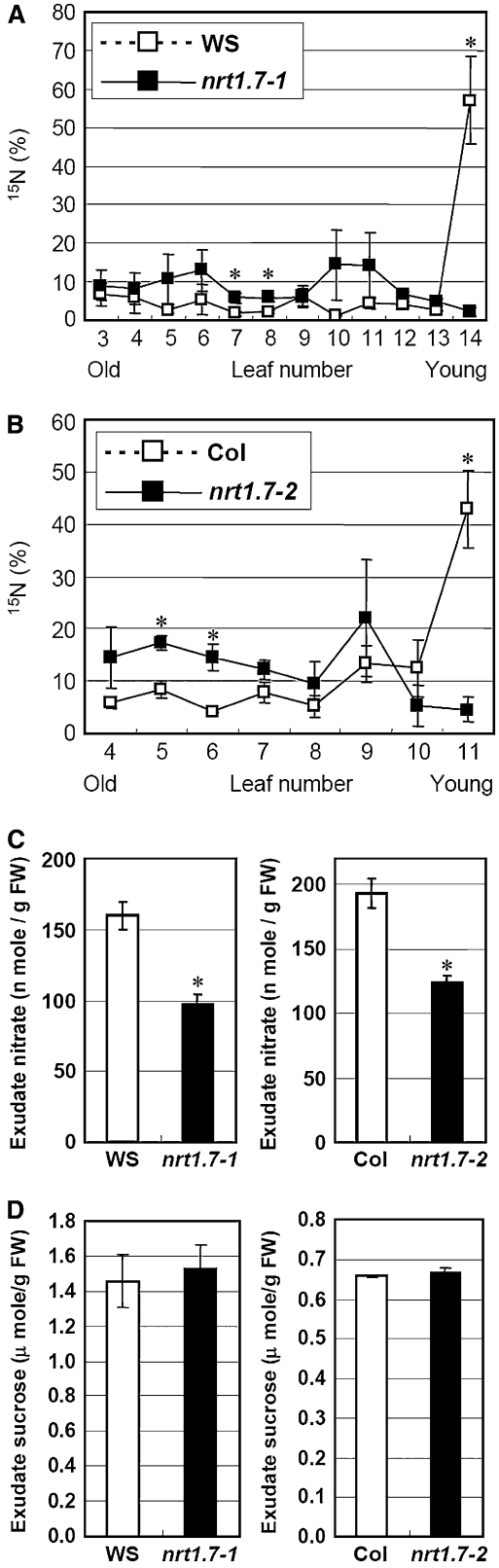

Figure 6. *nrt1.7* Mutants Are Defective in Remobilizing ^{15}N-Nitrate from Old to Sink Tissues.

(A) and **(B)** ^{15}N-nitrate tracing assay in the wild type and mutant. The 28- to 32-d-old plants grown in soil with full nutrient availability under 16-h photoperiod were used for ^{15}N-nitrate tracing. ^{15}N-nitrate was spotted on the oldest leaf, and after 20 h, the ^{15}N content was measured in different leaves. The amount of ^{15}N in each leaf is presented as the percentage of total ^{15}N in rosette leaves. Values are mean ± SE of three independent plants. *, Significant difference ($P < 0.01$) between the wild types and mutants.

(C) Nitrate contents in phloem exudates. Nitrate contents in phloem exudates of old leaf were lower in *nrt1.7* mutants. Values are means ± SE of three biological repeats. *, Significant difference ($P < 0.005$) between the wild types and mutants.

(D) Sucrose contents in phloem exudates. Sucrose content in the same phloem exudates of **(C)** were measured. There was no significant difference between the wild types and mutants. Values are means ± SE of three biological repeats.

provides genetic evidence for the involvement of nitrate remobilization in the ability to withstand nitrogen starvation. It will be interesting to see in the future if any QTL associated with NUE will be mapped to NRT1.7 orthologs in crop plants.

It is well documented that during leaf senescence, organic nitrogen derived from degraded protein will be remobilized to support the growth of young tissues (Masclaux-Daubresse et al., 2008). Our study of NRT1.7 indicates that inorganic nitrogen nitrate can also be remobilized from older leaves into nitrogen-demanding tissues. In addition to growth retardation upon long-term nitrogen starvation, mutants of *nrt1.7-2* also showed early senescence in older leaves when plants encountered nitrogen deficiency during the reproductive stage (see Supplemental Figure 7 online). Interestingly, such senescence was initiated from distal parts of the leaf, where expression of *NRT1.7* is initiated. The senescence could be caused by excess nitrate accumulation in older leaves or enhanced nitrogen demand signal from the reproductive tissues. The enhanced nitrogen demand signal may accelerate senescence to enhance proteolysis and remobilization of organic nitrogen into sink tissues. However, the early senescence phenotype was only observed in *nrt1.7-2* mutants (Col ecotype) but not in *nrt1.7-1* mutants (Ws ecotype) and thus may be due to different nitrogen use strategies in different *Arabidopsis* ecotypes.

Nitrate Remobilization Is Mediated by Phloem Transport

NRT1.7, responsible for remobilizing nitrate from older leaves to N-demanding tissues, is expressed in the sieve element and companion cell complex. Therefore, in contrast with root-to-shoot nitrate transport via the xylem, nitrate remobilization among different leaves and reproductive tissues is mediated by the phloem. Localization of NRT1.7 in the plasma membrane and the expression of *NRT1.7* in the sieve element and companion cell complex indicate that nitrate can be loaded into the phloem. Reduced nitrate content in the phloem exudates collected from older leaves of *nrt1.7* mutants suggest that nitrate itself is normally transported out of older leaves. Whether nitrate will be converted to some organic form as it travels from older leaves to N-demanding tissues is still an open question.

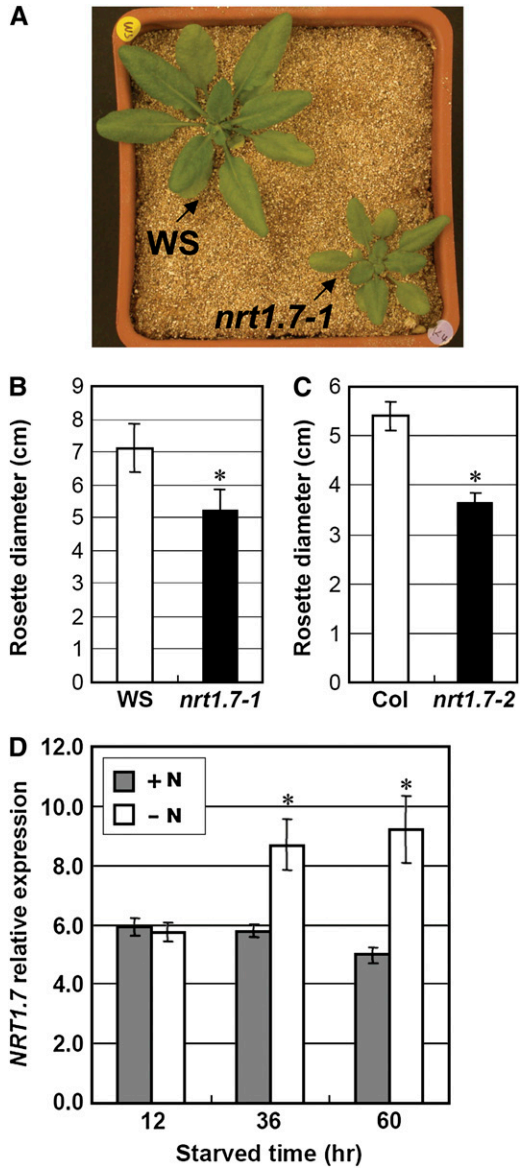

Figure 7. nrt1.7 Mutants Showed Growth Retardation upon Nitrogen Starvation.

(A) Representative 35-d-old plants grown with full nutrient for 10 d and then nitrogen starved for 25 d. Photos of 10-d-old plants before starvation are shown in Supplemental Figure 5 online.

(B) Rosette size of the wild type and *nrt1.7* mutants under nitrogen starvation. Values are means ± SD; $n = 5$ for Ws/*nrt1.7-1*, and $n = 4$ for Col/*nrt1.7-2*. Plants were grown with full nutrient for 10 d and then nitrogen starved for 25 d for Ws background and 15 d for Col background. *, Significant difference ($P < 0.005$) between the wild types and mutants.

(C) Quantitative RT-PCR analysis of *NRT1.7* expression in nitrogen starved plants. Plants were grown hydroponically for 34 d with full nutrients and then shifted to nitrogen-depleted medium for the time indicated. The relative expression level is the expression of *NRT1.7* normalized to that of *UBQ10*. Values are means ± SE of three biological repeats. *, Significant difference ($P < 0.005$) between full nutrient and nitrogen starvation.

Phloem-mediated nitrate remobilization could take advantage of the source-to-sink directed transport of phloem. Indeed, in the wild-type plant, the majority of ^{15}N-nitrate spotted on older leaves was transported directly to young leaves. Sometimes, a small amount of ^{15}N-nitrate spotted on old leaf was found to have leaked out into adjacent leaves. This leak transport to adjacent leaves was more obvious in *nrt1.7* mutants, when the function of the *NRT1.7* was blocked (Figures 6A and 6B). The leak or diffusion process could provide an alternative pathway to transport nitrate out of older leaves, but NRT1.7 is responsible for a superhighway to facilitate the rapid delivery of nitrate from older leaves to N-demanding tissues.

Comparison of Diurnal Regulation of NRT1.7 and Nitrate Reductase

Nitrate is assimilated by nitrate reductase in cytosol, and excess nitrate in the cell can be stored in the vacuole. Similar to the expression of nitrate reductase genes (Cheng et al., 1991), the expression level of *NRT1.7* was also diurnally regulated. However, the temporal pattern of *NRT1.7* was opposite to that of *NIA2* in that *NRT1.7* expression was highest at dusk, while *NIA2* was highest at dawn. The opposite diurnal patterns of *NRT1.7* and *NIA2* suggest that when nitrate reductase activity is downregulated during the night, excess nitrate in the leaf can be exported out by NRT1.7. Using different time periods for assimilation and export could ensure that the older leaves still get sufficient nitrate for assimilation to meet their own nitrogen demand, and only excess nitrate is transported out. For most plants, the amount of sucrose exported from the source leaf during the night is similar to or slightly lower than the amount exported during the day (Pate et al., 1979; Mitchell et al., 1992). The sucrose exported during the night comes from hydrolysis of starch stored during the day. Since nitrate remobilization and sucrose remobilization use the same path phloem for transport, and *NRT1.7* expression is upregulated by sucrose (see Supplemental Figure 8 online), nitrate remobilization might be an additional step of regulation for N-C balance.

METHODS

Functional Analysis of NRT1.7 in *Xenopus laevis* Oocytes

A full-length pNRT1.7 (At1g69870) clone was isolated from an *Arabidopsis thaliana* cDNA library (Elledge et al., 1991) using the NRT1.1 (CHL1) homology EST clone (clone ID 119P20) as a probe. The 1.9-kb full-length cDNA fragment of *NRT1.7* was subcloned into the pGEMHE vector (Liman et al., 1992) to generate pGEMHE-*NRT1.7*. The pGEMHE-NRT1.7 was linearized using *Nhe*I, and capped mRNA was transcribed in vitro using mMESSAGE mMACHINE kits (Ambion). Oocytes were injected with 100 ng of NRT1.7 cRNA as described previously (Tsay et al., 1993). Electrophysiological analyses of injected oocytes were performed as described previously (Huang et al., 1999). Nitrate uptake assays using ^{15}N-nitrate were performed as described previously using a continuous-flow isotope ratio mass spectrometer coupled with a carbon nitrogen elemental analyzer (ANCA-GSL MS; PDZ Europa; Lin et al., 2008), and oocytes injected with CHL1 cRNA (Liu et al., 1999) were used as a positive control.

Plant Growth Condition and *nrt1.7* Mutants

Unless otherwise indicated in the figure legend, most *Arabidopsis* plants used in this study were grown in soil containing compost:humus at a 3:1 ratio, at 22°C, with a 16-h photoperiod, and 60% relative humidity, irrigated with full nutrient using HYPONeX #2 fertilizer (Almagro et al., 2008) at final concentrations of 6 mM nitrate, 5.3 mM potassium, and 3.5 mM phosphate. For nitrogen starvation experiments, plants were grown in soil containing perlite:vermiculite at a 1:2 ratio and covered with a thin layer of fine vermiculite, irrigated with HYPONeX #2 fertilizer for 10 or 25 d as indicated in the figure legends, and then watered with a nitrogen-depleted solution containing 5 mM K_2HPO_4/KH_2PO_4, pH 5.5, and the basal nutrients (1 mM $MgSO_4$, 0.1 mM $FeSO_4$-EDTA, 0.5 mM $CaCl_2$, 50 μM H_3BO_3, 12 μM $MnSO_4$, 1 μM $ZnCl_2$, 1 μM $CuSO_4 \cdot 5H_2O$, and 0.2 μM $Na_2MoO_4 \cdot 2H_2O$). For phloem exudate collection and measurement of *NRT1.7* expression in response to starvation, plants were grown hydroponically in a solution containing 1 mM K_2HPO_4/KH_2PO_4 at pH 5.5, the basal nutrients described above, and with or without 1 mM NH_4NO_3. All experiments compared by wild-type and mutant plants were grown in the same pot.

The *nrt1.7-1* line was obtained from the ALPHA population (Ws ecotype) of T-DNA–tagged plants generated by the Arabidopsis Knockout Facility at the University of Wisconsin Biotech Center (Krysan et al., 1999). The primers used for PCR screening were JL202 (Lin et al., 2008) and the NRT1.7 forward primer (5′- CCACACCCACCATATATTATCTACTC-ACT-3′). The second mutant *nrt1.7-2* (SALK_053264) was provided by the Salk Institute Genomic Analysis Laboratory (Alonso et al., 2003).

Antibody and Immunoblots

The anti-NRT1.7 rabbit polyclonal antibody was generated using a peptide corresponding to the first N-terminal 50 amino acids. The cDNA fragment encoding the N-terminal 1 to 50 amino acids was amplified by PCR using primer pairs of forward 5′-gaattctaATGGTTTTG-GAGGATAG-3′ and reverse 5′-aaGCTTTTTCTCTACCTTCTCAG-3′, which introduced *Eco*RI and *Hin*dIII restriction sites, respectively, and subcloned into pGEX-KG in frame with the glutathione *S*-transferase (GST) to generate pGEX-KG-NRT1.7-N50. GST fusion protein was isolated from *Escherichia coli* (BL21) and purified by GST beads. Purified GST fusion protein was emulsified with Freund's adjuvant and injected into New Zealand rabbits according to the protocol of Spindler et al. (1984).

For protein immunoblot analysis, tissues were homogenized in ice-cold extraction buffer consisting of 15 mM Tris-HCl, pH 7.8, 250 mM sucrose, 1 mM EDTA, 2 mM DTT, 1 mM phenylmethylsulfonyl fluoride, 0.6% polyvinylpyrrolidone, and protease inhibitor cocktail (Roche). The homogenate was then centrifuged at 10,000*g* for 10 min, and the supernatant was collected in a chilled tube. The supernatant was centrifuged at 100,000*g* for 1 h, and then the pellet, the microsomal fraction, was dissolved in 4% SDS. Ten micrograms of protein were analyzed by SDS-PAGE. Detections were performed using the ECL protein gel blotting system (Amersham, GE Healthcare). Anti-NRT1.7, Anti-BiP, and horseradish peroxidase–labeled anti-rabbit IgG antibody were used at dilutions of 1:2000, 1:2000, and 1:10,000, respectively. Bands were detected by BioMax M_R film (Kodak) and quantified by VisionWorks analysis software from Ultra-Violet Products, and the signals were in linear range.

RT-PCR and Quantitative RT-PCR

The ImProm-II reverse transcriptase (Promega), oligo(dT) primers, and the RNA isolated from different developmental stages of leaves and flowers were used to synthesize the first-strand cDNAs. Primers across the intron of Histone were used to exclude genomic contamination. Primers specific for the *NRT1.7*, *NIA2*, and *UBQ10* gene were designed by ABI software. Quantitative PCR was performed with an AB7500 using Power SYBR Green (ABI System). The primers used were as follows: *Histone* (forward, 5′-AACCACTGGAGGAGTCAAGA-3′; reverse, 5′-CAATTAAGCACGTTCTCCTCT-3′), *NRT1.7* (forward, 5′-CAACAGT-CAGTTTCCAGAGCACAT-3′; reverse, 5′-CGACAGTCACAAGGAAACTAC-TAAGGTA-3′), *NIA2* (forward, 5′-AGGATCCAGAGGATGAGACTGAAA-3′; reverse, 5′-CCTTAGCTGATTCCACTACGTACCA-3′), and *UBQ10* (forward, 5′-AGAAGTTCAATGTTTCGTTTCATGTAA-3′; reverse, 5′-GAACG-GAAACATAGTAGAACACTTATTCA-3′).

Promoter-GUS Analysis

A 1.35-kb genomic fragment of *NRT1.7* promoter (−1346 to +3 bp) was generated by PCR using the primers forward 5′-gtcgaCAAATATTTTCC-TATAACATA-3′ and reverse 5′-ggatcctCATCTCTAAGATATTACT-3′, cut with *Xba*I and *Bam*HI, and then inserted in frame in front of *uidA* (GUS) of pBI101. Plant trasnsformation was performed as previously described (Clough and Bent, 1998). Homozygous transgenic plants (T3) of 28- to 32-d-old cultivated in full nutrient soil were used for GUS histochemical assay, using GUS staining as described previously (Lagarde et al., 1996). Cross sections of 2-μm thickness were prepared using a microtome (Ultracut E; Reichert-Jung) from tissues embedded in medium-grade LR White (London Resin Company).

Whole-Mount Immunolocalization

To enhance the specificity, anti-NRT1.7 antiserum was affinity purified first by the antigen used to raise antiserum (a GST fusion of the first 50 amino acids of NRT1.7) and then by HA-tagged full-length NRT1.7 protein. Older (40 d old) Col and *nrt1.7-2* leaves were used for whole-mount immunohybridization (Bauwens et al., 1994). For antigen retrieval before hybridization, tissues were incubated in 1 mM EDTA at 95°C for 5 min and then blocked for 2 h in blocking buffer (50 mM Tris-HCl, pH 7.5, 150 mM NaCl, and 1% gelatin). After 36 h incubation with affinity-purified anti-NRT1.7 antiserum in 1:10 dilution at 4°C, tissues were washed three times with blocking buffer and then hybridized with Alexa Fluor 488 goat anti-rabbit IgG (Molecular Probes) in 1:500 dilution. Green fluorescence was detected by a Zeiss LSM META-510 microscope with excitation at 488 nm. Fluorescence emission signals were detected using a band-pass filter of 505 to 530 nm. Sieve plates were stained with 0.2% aniline blue (Water Blue; Fluka) in 50 mM Na-PO_4 buffer for 30 min. Aniline blue fluorescence was detected with an excitation light of 405 nm and band-pass filter of 420 to 480 nm.

GFP Fusion and Subcellular Localization

To construct the plasmid encoding NRT1.7-GFP fusion protein, *NRT1.7* cDNA was amplified by PCR using the primers *NRT1.7NF* (5′-tctagA-TGGTTTTGGAGGATAGA-3′) and *NRT1.7NR* (5′-ggatccCATTTCATC-GATTTCTT-3′); the former primer introduces a *Xba*I restriction site, and the latter removes the stop codon and introduces a *Bam*HI restriction site. The amplified DNA fragment was then cloned in frame in front of the GFP coding region in the vector 326-GFP (Lee et al., 2001), leading to the final pNRT1.7-GFP construct under the control of the 35S promoter. The fusion linker between NRT1.7 and GFP contained seven amino acids (YIQGDIT). To construct the plasmid encoding pGFP-NRT1.7 fusion protein, the *NRT1.7* cDNA was amplified by PCR with primers *NRT1.7CF* (5′-ctcgagATGGTTTTGGAGGATAGA-3′) and *NRT1.7CR* (5′-ctcgag-TCATTTCATCGATTTCTT-3′), which introduced *Xho*I restriction sites, and then cloned in frame into vector 326-GFP-nt (no termination codon) behind GFP. The fusion linker between GFP and NRT1.7 contained 13 amino acids (PRAIKLIDTVDLE). The vector 326-GFP was used as a free GFP control.

Transient transformation of *Arabidopsis* protoplasts with polyethylene glycol was performed as described previously (Yoo et al., 2007). After transformation, protoplasts were incubated overnight at room temperature under illumination (25 μE) and then observed by a Zeiss LSM510 microscope with excitation at 488 nm. Fluorescence emission signals were detected using a band-pass filter of 505 to 530 nm for GFP and a long-pass filter of 650 nm for the far-red autofluorescence of the chloroplast.

Measurement of the Nitrate Content in *Arabidopsis* Leaves

The rosette leaves were collected and immediately frozen in liquid nitrogen. To extract nitrate, samples were boiled in water (100 μL/mg FW) and then freeze-thawed once. After filtering through 0.2-μm polyvinylidene fluoride membrane (Pall Corporation), nitrate content of the samples was determined by HPLC using a PARTISIL 10 SAX (strong anion exchanger) column (Whatman) and 50 mM phosphate buffer, pH 3.0, as the mobile phase.

^{15}N-Nitrate Tracing Assay

Three days after bolting, 10 μL of 50 mM $K^{15}NO_3$ with a 98% atom excess of ^{15}N was spotted on distal parts of the oldest leaf. Approximately 20 h after spotting, individual leaves were collected and dried at 80°C for 24 h, at which point ^{15}N content was analyzed as described previously using a continuous-flow isotope ratio mass spectrometer coupled with a carbon nitrogen elemental analyzer (ANCA-GSL MS; PDZ Europa) (Lin et al., 2008).

Collection and Analysis of Phloem Exudates

Three days after bolting, phloem exudates were collected from excised leaves using procedures modified from the protocol previously described (Deeken et al., 2008). The third and fourth leaves were cut, and the tip of the petiole was recut in EDTA buffer (5 mM Na_2EDTA, pH 7.5, osmotically adjusted to 270 mosmol with sorbitol) with fresh razor blades without wounding. The leaves were washed with a large volume of sterile EDTA buffer to remove contaminants and then placed in 200 μL new EDTA buffer. During phloem sap exudation, the leaves were illuminated (25 μE) and incubated in a chamber. After 1 h of bleeding, the buffer solution containing phloem exudates was analyzed for nitrate and sugar content. Nitrate content was measured by HPLC as described above. Sucrose and glucose content were measured by the DNS method as described elsewhere (Bernfeld, 1995).

Accession Numbers

Sequence data from this article can be found in the GenBank/EMBL data libraries under the following accession numbers: At1g69870 (NRT1.7), At1g12110 (CHL1, NRT1.1), At1g69850 (NRT1.2), At3g21670 (NTP3, NRT1.3) At2g26690 (NTP2, NRT1.4), At1g32450 (NRT1.5), At1g27080 (NRT1.6), At1g08090 (NRT2.1), At1g08100 (NRT2.2), At1g12940 (NRT2.7), At3g45650 (NAXT1) At3g54140 (PTR1), At2g02040 (PTR2), At5g46050 (PTR3), At5g40890 (CLCa), At5g40780 (LHT1), At4g05320 (UBQ10), At1g22710 (SUC2), At4g22200 (AKT2), At4g40040 (Histone), and At5g42020 (BiP).

Supplemental Data

The following materials are available in the online version of this article.

Supplemental Figure 1. Amino Acid Sequence Alignment of the *Arabidopsis* Nitrate Transporters in NRT1 Family.

Supplemental Figure 2. *NRT1.7* Expression Levels in Vegetative Tissues.

Supplemental Figure 3. Continuous Confocal Images of NRT1.7 Whole-Mount Immunostaining.

Supplemental Figure 4. The Ratio of Nitrate Content in Each Leaf.

Supplemental Figure 5. *nrt1.7* Mutants Do Not Show Growth Defect before Nitrogen Starvation.

Supplemental Figure 6. Expression of *NRT1.7* Is Regulated by Nitrogen Starvation.

Supplemental Figure 7. Early Senescence in *nrt1.7-2* Mutant with Late Nitrogen Starvation.

Supplemental Figure 8. Expression of *NRT1.7* Is Regulated by Sucrose.

Supplemental Data Set 1. Text File Corresponding to the Alignment in Supplemental Figure 1.

ACKNOWLEDGMENTS

We thank Sue-Pin Li from our confocal core facility for her help with the GFP images and GUS sections and Chi-Chou Chiu for his help with amino acid sequence alignment. Anti-BiP antibody was kindly provided by Masayoshi Maeshima (Nagoya University); 326-GFP and 326-GFP-nt vectors were gifts from Inhwan Hwang (Pohang University of Science and Technology). We thank Harry Wilson and Miranda Loney of Academia Sinica for English editing. This work was supported by grants from the National Science Council (NSC 97-2311-B001-009) and the Institute of Molecular Biology, Academia Sinica, Taipei, Taiwan.

Received April 6, 2009; revised August 13, 2009; accepted August 20, 2009; published September 4, 2009.

REFERENCES

Allen, S., and Smith, J. (1986). Ammonium nutrition in *Ricinus communis*: Its effect on plant growth and the chemical composition of the whole plant, xylem and phloem saps. J. Exp. Bot. **37:** 1599–1610.

Almagro, A., Lin, S.H., and Tsay, Y.F. (2008). Characterization of the *Arabidopsis* nitrate transporter NRT1.6 reveals a role of nitrate in early embryo development. Plant Cell **20:** 3289–3299.

Alonso, J.M., et al. (2003). Genome-wide insertional mutagenesis of *Arabidopsis thaliana.* Science **301:** 653–657.

Bauwens, S., Katsanis, K., Van Montagu, M., Van Oostveldt, P., and Engler, G. (1994). Procedure for whole mount fluorescence *in situ* hybridization of interphase nuclei on *Arabidopsis thaliana.* Plant J. **6:** 123–131.

Bernfeld, P. (1995). Amylases, α and β. Methods Enzymol. **1:** 149–158.

Caputo, C., and Barneix, A. (1997). Export of amino acids to the phloem in relation to N supply in wheat. Physiol. Plant. **101:** 853–860.

Cheng, C.L., Acedo, G.N., Dewdney, J., Goodman, H.M., and Conkling, M.A. (1991). Differential expression of the two Arabidopsis nitrate reductase genes. Plant Physiol. **96:** 275–279.

Chiu, C.C., Lin, C.S., Hsia, A.P., Su, R.C., Lin, H.L., and Tsay, Y.F. (2004). Mutation of a nitrate transporter, AtNRT1:4, results in a reduced petiole nitrate content and altered leaf development. Plant Cell Physiol. **45:** 1139–1148.

Chopin, F., Orsel, M., Dorbe, M.F., Chardon, F., Truong, H.N., Miller, A.J., Krapp, A., and Daniel-Vedele, F. (2007). The *Arabidopsis* AtNRT2.7 nitrate transporter controls nitrate content in seeds. Plant Cell **19:** 1590–1602.

Clough, S.J., and Bent, A.F. (1998). Floral dip: A simplified method for *Agrobacterium*-mediated transformation of *Arabidopsis thaliana.* Plant J. **16:** 735–743.

De Angeli, A., Monachello, D., Ephritikhine, G., Frachisse, J., Thomine, S., Gambale, F., and Barbier-Brygoo, H. (2006). The nitrate/proton antiporter AtCLCa mediates nitrate accumulation in plant vacuoles. Nature **442:** 939–942.

Deeken, R., Ache, P., Kajahn, I., Klinkenberg, J., Bringmann, G., and Hedrich, R. (2008). Identification of *Arabidopsis thaliana* phloem RNAs provides a search criterion for phloem-based transcripts hidden in complex datasets of microarray experiments. Plant J. **55:** 746–759.

Elledge, S.J., Mulligan, J.T., Ramer, S.W., Spottswood, M., and Davis, R.W. (1991). Lambda YES: A multifunctional cDNA expression vector for the isolation of genes by complementation of yeast and *Escherichia coli* mutations. Proc. Natl. Acad. Sci. USA **88:** 1731–1735.

Filleur, S., Dorbe, M., Cerezo, M., Orsel, M., Granier, F., Gojon, A., and Daniel-Vedele, F. (2001). An Arabidopsis T-DNA mutant affected in *Nrt2* genes is impaired in nitrate uptake. FEBS Lett. **489:** 220–224.

Forde, B.G. (2000). Nitrate transporters in plants: structure, function and regulation. Biochim. Biophys. Acta **1465:** 219–235.

Good, A.G., Shrawat, A.K., and Muench, D.G. (2004). Can less yield more? Is reducing nutrient input into the environment compatible with maintaining crop production? Trends Plant Sci. **9:** 597–605.

Hayashi, H., and Chino, M. (1985). Nitrate and other anions in the rice phloem sap. Plant Cell Physiol. **26:** 325–330.

Hayashi, H., and Chino, M. (1986). Collection of pure phloem sap from wheat and its chemical composition. Plant Cell Physiol. **27:** 1387–1393.

Hechenberger, M., Schwappach, B., Fischer, W., Frommer, W., Jentsch, T., and Steinmeyer, K. (1996). A family of putative chloride channels from Arabidopsis and functional complementation of a yeast strain with a CLC gene disruption. J. Biol. Chem. **271:** 33632–33638.

Hirel, B., Bertin, P., Quillere, I., Bourdoncle, W., Attagnant, C., Dellay, C., Gouy, A., Cadiou, S., Retailliau, C., Falque, M., and Gallais, A. (2001). Towards a better understanding of the genetic and physiological basis for nitrogen use efficiency in maize. Plant Physiol. **125:** 1258–1270.

Hocking, P.J. (1980). The composition of phloem exudate and xylem sap from tree tobacco (*Nicotiana glauca* Grah.). Ann. Bot. (Lond.) **45:** 633–643.

Hortensteiner, S., and Feller, U. (2002). Nitrogen metabolism and remobilization during senescence. J. Exp. Bot. **53:** 927–937.

Huang, N.C., Liu, K.H., Lo, H.J., and Tsay, Y.F. (1999). Cloning and functional characterization of an *Arabidopsis* nitrate transporter gene that encodes a constitutive component of low-affinity uptake. Plant Cell **11:** 1381–1392.

Ishida, H., Nishimori, Y., Sugisawa, M., Makino, A., and Mae, T. (1997). The large subunit of ribulose-1,5-bisphosphate carboxylase/oxygenase is fragmented into 37-kDa and 16-kDa polypeptides by active oxygen in the lysates of chloroplasts from primary leaves of wheat. Plant Cell Physiol. **38:** 471–479.

Jukanti, A., and Fischer, A. (2008). A high-grain protein content locus on barley (*Hordeum vulgare*) chromosome 6 is associated with increased flag leaf proteolysis and nitrogen remobilization. Physiol. Plant. **132:** 426–439.

Kato, Y., Murakami, S., Yamamoto, Y., Chatani, H., Kondo, Y., Nakano, T., Yokota, A., and Sato, F. (2004). The DNA-binding protease, CND41, and the degradation of ribulose-1,5-bisphosphate carboxylase/oxygenase in senescent leaves of tobacco. Planta **220:** 97–104.

Kichey, T., Hirel, B., Heumez, E., Dubois, F., and Le Gouis, J. (2007). In winter wheat (*Triticum aestivum L.*), post-anthesis nitrogen uptake and remobilisation to the grain correlates with agronomic traits and nitrogen physiological markers. Field Crops Res. **102:** 22–32.

Kiefer, I.W., and Slusarenko, A.J. (2003). The pattern of systemic acquired resistance induction within the Arabidopsis rosette in relation to the pattern of translocation. Plant Physiol. **132:** 840–847.

Krysan, P.J., Young, J.C., and Sussman, M.R. (1999). T-DNA as an insertional mutagen in *Arabidopsis*. Plant Cell **11:** 2283–2290.

Lagarde, D., Basset, M., Lepetit, M., Conejero, G., Gaymard, F., Astruc, S., and Grignon, C. (1996). Tissue-specific expression of Arabidopsis *AKT1* gene is consistent with a role in K^+ nutrition. Plant J. **9:** 195–203.

Lansing, A.J., and Franceschi, V.R. (2000). The paraveinal mesophyll: A specialised path for intermediary transfer of assimilates in legume leaves. Aust. J. Plant Physiol. **27:** 757–767.

Lee, Y.J., Kim, D.H., Kim, Y.-W., and Hwang, I. (2001). Identification of a signal that distinguishes between the chloroplast outer envelope membrane and the endomembrane system in vivo. Plant Cell **13:** 2175–2190.

Li, W., Wang, Y., Okamoto, M., Crawford, N.M., Siddiqi, M.Y., and Glass, A.D. (2007). Dissection of the AtNRT2.1:AtNRT2.2 inducible high-affinity nitrate transporter gene cluster. Plant Physiol. **143:** 425–433.

Liman, E.R., Tytgat, J., and Hess, P. (1992). Subunit stoichiometry of a mammalian K^+ channel determined by construction of multimeric cDNAs. Neuron **9:** 861–871.

Lin, S.H., Kuo, H.F., Canivenc, G., Lin, C.S., Lepetit, M., Hsu, P.K., Tillard, P., Lin, H.L., Wang, Y.Y., Tsai, C.B., Gojon, A., and Tsay, Y.F. (2008). Mutation of the *Arabidopsis* NRT1.5 nitrate transporter causes defective root-to-shoot nitrate transport. Plant Cell **20:** 2514–2528.

Little, D.Y., Rao, H., Oliva, S., Daniel-Vedele, F., Krapp, A., and Malamy, J.E. (2005). The putative high-affinity nitrate transporter NRT2.1 represses lateral root initiation in response to nutritional cues. Proc. Natl. Acad. Sci. USA **102:** 13693–13698.

Liu, K., and Tsay, Y. (2003). Switching between the two action modes of the dual-affinity nitrate transporter CHL1 by phosphorylation. EMBO J. **22:** 1005–1013.

Liu, K.H., Huang, C.Y., and Tsay, Y.F. (1999). CHL1 is a dual-affinity nitrate transporter of *Arabidopsis* involved in multiple phases of nitrate uptake. Plant Cell **11:** 865–874.

Masclaux-Daubresse, C., Reisdorf-Cren, M., and Orsel, M. (2008). Leaf nitrogen remobilisation for plant development and grain filling. Plant Biol (Stuttg) **10** (suppl. 1): 23–36.

Matile, P., Schellenberg, M., and Peisker, C. (1992). Production and release of a chlorophyll catabolite in isolated senescent chloroplasts. Planta **187:** 230–235.

Mickelson, S., See, D., Meyer, F.D., Garner, J.P., Foster, C.R., Blake, T.K., and Fischer, A.M. (2003). Mapping of QTL associated with nitrogen storage and remobilization in barley (*Hordeum vulgare* L.) leaves. J. Exp. Bot. **54:** 801–812.

Mitchell, D., Gadus, M., and Madore, M. (1992). Patterns of assimilate production and translocation in muskmelon (*Cucumis melo* L.). I. Diurnal patterns. Plant Physiol. **99:** 959–965.

Mitsuhashi, W., Craftsbrandner, S.J., and Feller, U. (1992). Ribulose-1,5-bis-phosphate carboxylase oxygenase degradation in isolated pea-chloroplasts incubated in the light or in the dark. J. Plant Physiol. **139:** 653–658.

Orsel, M., Filleur, S., Fraisier, V., and Daniel-Vedele, F. (2002). Nitrate transport in plants: Which gene and which control? J. Exp. Bot. **53:** 825–833.

Pate, J., Atkins, C., Hamel, K., McNeil, D., and Layzell, D. (1979). Transport of organic solutes in phloem and xylem of a nodulated legume. Plant Physiol. **63:** 1082–1088.

Pate, J., Sharkey, P., and Lewis, O. (1975). Xylem to phloem transfer of solutes in fruiting shoots of legumes, studied by a phloem bleeding technique. Planta **122:** 11–26.

Peoples, M.B., Freney, J.R., and Mosier, A.R. (1995). Minimizing gaseous losses of nitrogen. In Nitrogen Fertilizer in the Environment, P.E. Bacon, ed (New York: Marcel Dekker), pp. 565–606.

Richard-Molard, C., Krapp, A., Brun, F., Ney, B., Daniel-Vedele, F., and Chaillou, S. (2008). Plant response to nitrate starvation is determined by N storage capacity matched by nitrate uptake capacity in two Arabidopsis genotypes. J. Exp. Bot. **59:** 779–791.

Rochat, C., and Boutin, J.P. (1991). Metabolism of phloem-borne amino-acids in maternal tissues of fruit of nodulated or nitrate-fed pea-plants (*Pisum sativum* L). J. Exp. Bot. **42:** 207–214.

Rossato, L., Laine, P., and Ourry, A. (2001). Nitrogen storage and remobilization in *Brassica napus* L. during the growth cycle: Nitrogen fluxes within the plant and changes in soluble protein patterns. J. Exp. Bot. **52:** 1655–1663.

Roulin, S., and Feller, U. (1998). Dithiothreitol triggers photooxidative stress and fragmentation of the large subunit of ribulose-1,5-bisphosphate carboxylase/oxygenase in intact pea chloroplasts. Plant Physiol. Biochem. **36:** 849–856.

Schiltz, S., Munier-Jolain, N., Jeudy, C., Burstin, J., and Salon, C. (2005). Dynamics of exogenous nitrogen partitioning and nitrogen remobilization from vegetative organs in pea revealed by ^{15}N in vivo labeling throughout seed filling. Plant Physiol. **137:** 1463–1473.

Segonzac, C., Boyer, J.C., Ipotesi, E., Szponarski, W., Tillard, P., Touraine, B., Sommerer, N., Rossignol, M., and Gibrat, R. (2007). Nitrate efflux at the root plasma membrane: identification of an *Arabidopsis* excretion transporter. Plant Cell **19:** 3760–3777.

Simpson, R.J., Lambers, H., and Dalling, M.J. (1983). Nitrogen redistribution during grain growth in wheat (*Triticum aestivum* L.). IV. Development of a quantitative model of the translocation of nitrogen to the grain. Plant Physiol. **71:** 7–14.

Smith, J., and Milburn, J. (1980). Osmoregulation and the control of phloem-sap composition in *Ricinus communis* L. Planta **148:** 28–34.

Spindler, K.R., Rosser, D.S., and Berk, A.J. (1984). Analysis of adenovirus transforming proteins from early regions 1A and 1B with antisera to inducible fusion antigens produced in *Escherichia coli.* J. Virol. **49:** 132–141.

Tsay, Y.F., Chiu, C.C., Tsai, C.B., Ho, C.H., and Hsu, P.K. (2007). Nitrate transporters and peptide transporters. FEBS Lett. **581:** 2290–2300.

Tsay, Y.F., Schroeder, J.I., Feldmann, K.A., and Crawford, N.M. (1993). The herbicide sensitivity gene CHL1 of Arabidopsis encodes a nitrate-inducible nitrate transporter. Cell **72:** 705–713.

Turgeon, R., and Webb, J.A. (1973). Leaf development and phloem transport in *Cucurbita pepo*: Transition from import to export. Planta **113:** 179–191.

Wang, R., Liu, D., and Crawford, N.M. (1998). The Arabidopsis CHL1 protein plays a major role in high-affinity nitrate uptake. Proc. Natl. Acad. Sci. USA **95:** 15134–15139.

Wendler, R., Carvalho, P., Pereira, J., and Millard, P. (1995). Role of nitrogen remobilization from old leaves for new leaf growth of Eucalyptus globulus seedlings. Tree Physiol. **15:** 679–683.

Yoo, S.D., Cho, Y.H., and Sheen, J. (2007). Arabidopsis mesophyll protoplasts: A versatile cell system for transient gene expression analysis. Nat. Protoc. **2:** 1565–1572.